

# Grappa: Gradient-Only Communication for Scalable Graph Neural Network Training

Chongyang Xu

Max Planck Institute for Software  
Systems (MPI-SWS)  
Saarbrücken, Germany  
cxu@mpi-sws.org

Christoph Siebenbrunner

Vienna University of Economics and  
Business (WU)  
Vienna, Austria  
christoph.siebenbrunner@wu.ac.at

Laurent Bindschaedler

Max Planck Institute for Software  
Systems (MPI-SWS)  
Saarbrücken, Germany  
bindsch@mpi-sws.org

## Abstract

Cross-partition edges dominate the cost of distributed GNN training: fetching remote features and activations per iteration overwhelms the network as graphs deepen and partition counts grow. Grappa is a distributed GNN training framework that enforces *gradient-only communication*: during each iteration, partitions train in isolation and exchange only gradients for the global update. To recover accuracy lost to isolation, Grappa (i) periodically *repartitions* to expose new neighborhoods and (ii) applies a lightweight *coverage-corrected gradient aggregation* inspired by importance sampling. We prove the corrected estimator is asymptotically unbiased under standard support and boundedness assumptions, and we derive a batch-level variant for compatibility with common deep-learning packages that minimizes mean-squared deviation from the ideal node-level correction. We also introduce a shrinkage version that improves stability in practice. Empirical results on real and synthetic graphs show that Grappa trains GNNs 4 $\times$  faster on average (up to 13 $\times$ ) than state-of-the-art systems, achieves better accuracy especially for deeper models, and sustains training at the trillion-edge scale on commodity hardware. Grappa is model-agnostic, supports full-graph and mini-batch training, and does not rely on high-bandwidth interconnects or caching.

## 1 Introduction

Graph Neural Networks (GNNs) are a widespread class of machine learning models that learn representations from graph-structured data. GNNs power applications in science, social networks, commerce, and finance [10, 14, 21, 22, 27, 38, 51]. However, as graphs and models grow, distributed training encounters a network communication bottleneck, creating a need for efficient, scalable, and distributed GNN training. This paper addresses that need with a training framework that drastically reduces the communication bottleneck and is *model-agnostic, theory-backed, and empirically validated*.

Distributed GNN training partitions the sparse graph and the dense per-node feature vectors to fit memory and exploit parallelism. Training is iterative: each iteration runs a  $k$ -layer forward pass that performs message passing, where each node aggregates and transforms neighbor features into hidden activations, followed by a backward pass that computes gradients, and finally a synchronized update aggregates them

across replicas. Partitioning breaks edges, so when the forward pass follows a cross-partition edge, the trainer must fetch the remote endpoint’s feature at the first layer and the neighbor’s activation at deeper layers. As partition counts or model depth increase, these per-iteration remote fetches become the dominant cost, saturate the network, and throttle scalability. Mini-batch sampling [7, 33] reduces computation, but not cross-partition reads: the required neighbors still lie elsewhere. High-speed interconnects, such as RDMA or NVLink, can help; however, they are costly to deploy at scale and can introduce imbalance [6, 26, 37]. Caching reduces traffic by reusing fetched data, but it increases memory pressure and complexity [9, 34, 50]. Therefore, current strategies to address this performance bottleneck remain inadequate.

This paper introduces Grappa, a model-agnostic distributed framework for scalable GNN training on large graphs. Grappa *eliminates all cross-partition neighbor traffic*: in each iteration, partitions train in isolation and exchange only gradients (*gradient-only communication*). This approach reduces communication and synchronization overhead without specialized interconnects or caching-induced memory pressure. Moreover, partition independence within an iteration allows phase-parallel execution, which trades time for capacity by training only a subset of partitions per phase.

While this strategy minimizes communication costs, it introduces a new challenge: a potential decrease in model accuracy due to restricted sample diversity, as each partition only sees its local information. To recover accuracy, Grappa combines (1) *dynamic repartitioning* across groups of epochs (super-epochs) to expose new neighborhoods and (2) *coverage-corrected gradient aggregation*, a batch-level importance weighting that compensates for isolation-induced sampling bias. Intuitively, repartitioning is more cost-effective than on-the-fly neighbor fetches because the input graph is typically far smaller than the volume of per-iteration intermediate activations that would otherwise be exchanged.

**Formal guarantees.** We derive a batch-level corrected gradient estimator and prove it is *asymptotically unbiased* under standard support and boundedness conditions. We also show that, among all ways to rescale a batch with a single number, our choice makes the corrected batch gradient as close as possible (on average) to the ideal importance-weighted gradient (i.e., it minimizes average squared error).

We have implemented Grappa and evaluated its performance in our cluster. Across real-world and RMAT graph datasets, Grappa achieves  $4\times$  average speedup (up to  $13\times$ ) over state-of-the-art systems, improves test accuracy for deeper models, scales near-linearly to 64 partitions, and trains a trillion-edge graph in phase-parallel mode on a single commodity server.

**Terminology.** We use *gradient-only communication* to mean that there is no cross-partition exchange of features or activations during forward or backward passes; only gradients are synchronized across participating replicas.

The paper makes the following contributions:

- *Gradient-only communication*: a data-parallel scheme that eliminates cross-partition neighbor fetches within an iteration; only gradients are aggregated.
- *Theory-backed accuracy recovery*: dynamic repartitioning plus batch-level coverage-corrected aggregation. We prove an asymptotically unbiased node-level estimator and show that the batch-level variant minimizes the mean squared deviation from the ideal.
- *Flexible execution*: phase-parallel execution mode that trades time for capacity, allowing single-machine training at the trillion-edge scale.
- *Implementation and evaluation*: Grappa supports full-graph and mini-batch training and shows superior performance, accuracy, and scalability over current systems.

## 2 Background & Motivation

**GNNs 101.** A Graph Neural Network (GNN) takes a sparse graph (vertices, edges) with dense node features and learns node (and edge/graph) representations that encode both structure and features for downstream tasks. A  $k$ -layer forward pass performs message passing, so each node aggregates and transforms information from its neighbors and reaches  $k$  hops. Two execution modes are common: *full-graph* (all nodes and edges participate each iteration) and *mini-batch sampling* (sample target nodes and their multi-hop neighborhoods). Training is *iterative*: every iteration runs a forward pass, computes gradients via backpropagation, and updates parameters with gradient descent.

**Requirements and Goals.** Efficient training on large graphs requires a *distributed* system that provides sufficient *capacity* (graph, features, and intermediate states in aggregate memory) and that *parallelizes* computation across partitions to reduce training time. Given the compute intensity of deep models, *accelerators* (GPUs) are essential. Our goal is a *model-agnostic* system that is not tied to a specific GNN architecture, and that targets *ever-larger* graph datasets.

**Capacity Limits.** Pure GPU full-graph training is often infeasible at scale due to limited High-Bandwidth Memory (HBM). For example, an H100 has 80 GB, and even an 8-GPU node offers  $<640$  GB for *all* topology, features, parameters,

and activations [42, 44]. Several common datasets exceed this budget [19, 29]. Mini-batch sampling can offload graphs to CPU memory, but this merely shifts the capacity bottleneck to DRAM and I/O contention.

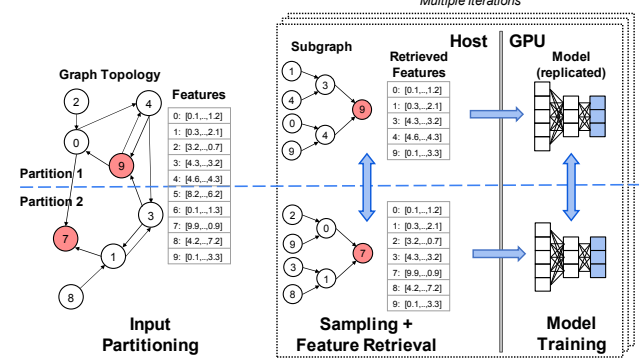


**Figure 1.** Sampling-based data-parallel GNN training. Each iteration samples multi-hop neighborhoods across *partitions* and aggregates gradients. Following cross-partition edges triggers remote feature/activation fetches, which dominate per-iteration cost at scale.

**Graph Partitioning.** Training a GNN on a large graph requires splitting the topology and features into partitions that are processed individually, as shown in Figure 1. This data-parallel training approach replicates the model and aggregates gradients. However, when the graph is partitioned, message passing must follow edges that cross partitions, forcing remote feature/hidden-state fetches during each iteration. As shown in Table 1, *cross-partition neighbor traffic* (features/activations) grows with graph size, number of partitions, and depth, and quickly becomes a significant bottleneck. Moreover, computing partitions that both balance the load and reduce edge cuts is itself expensive and difficult [5], and any imbalance further amplifies the effects of communication and stragglers.

Partition	Dataset	2 parts.	4 parts.	8 parts.
Random	Reddit	6,106 MB	9,216 MB	10,832 MB
	OGBN-Pr	21,448 MB	32,160 MB	37,682 MB
METIS	Reddit	3,264 MB	5,180 MB	5,512 MB
	OGBN-Pr	5,000 MB	10,120 MB	11,072 MB

**Table 1.** Per-partition neighbor traffic during a single training epoch (3-layer model) versus number of partitions. Datasets are in Table 2. Inputs are  $<1$  GB.

**Why Common Fixes Fall Short.** High-quality partitions (e.g., METIS [18]) reduce edge cuts but add heavy preprocessing and memory. Sampling lowers compute, but not the need to retrieve remote neighbors [7, 33]. Fast interconnects such as NVLink/RDMA [6, 26, 37] help within a node, yet gains do not generalize to clusters: when traffic leaves NVLink islands and falls back to PCIe or the network, epoch times balloon (e.g.,  $>11\times$  on OGBN-Pa and up to  $16\times$  on Reddit with MGG [1, 45]). Achieving uniform NVLink-class

bandwidth across nodes demands specialized switching and strict topologies, which is technically challenging and expensive. Caching [9, 34, 50] reduces traffic but consumes scarce HBM/DRAM and adds complexity. Thus, while existing approaches offer partial relief, the core tension between high capacity and cross-partition network traffic remains.

### 3 The Grappa Design

We begin with an overview of the system and its design principles (§3.1). Then, we introduce Grappa’s isolated training strategy (§3.2), its approach to dynamic repartitioning (§3.3), its sampling bias correction (§3.4), the training controller along with its heuristic for switching partitions (§3.5), and its phase-parallel training mode (§3.6).

#### 3.1 Overview

Grappa aims to efficiently train GNNs on large input graphs in a distributed, data-parallel fashion. Grappa supports both full-graph and sampling-based training modes (§2), although we focus mostly on sampling-based training as it offers superior scalability. Grappa divides the input graph and its features into partitions. Each partition is stored in CPU memory and loaded into GPU for training alongside the model. In the sampling-based training mode, we use the CPU to sample from the training nodes in the local partition to form mini-batches and load each batch into the GPU.

Unlike conventional GNN training, whether executing in full-graph or sampling mode, Grappa restricts graph access to the local partition only, preventing any data exchange along edges spanning multiple partitions, thereby executing training on each partition in complete isolation (§3.2). This strategy *eliminates cross-partition exchange of features or activations within an iteration*; cross-partition communication is *gradient-only*, which yields significant performance gains.

Grappa supports all GNN models compatible with other state-of-the-art systems, maintaining similar or improving accuracy but with lower training time. These speedups are primarily due to reduced communication and synchronization overheads, as we will show in Section 5. Moreover, due to its unique approach of processing partitions independently, Grappa achieves high flexibility in managing the overall training process. Since training on each partition can be performed separately from the others, there is no longer a need for concurrent data-parallel training of all partitions. Instead, it is enough for training on partitions to occur *conceptually in parallel*. Within each phase, gradients are synchronized across the active replicas, and across phases, we carry optimizer state forward. As a result, depending on available resources, Grappa can train some partitions sequentially, seamlessly trading training time for capacity (§3.6).

Figure 2 illustrates the workflow of Grappa as it trains a two-layer GNN model on an example input graph in sampling mode. Training is organized in super-epochs, each

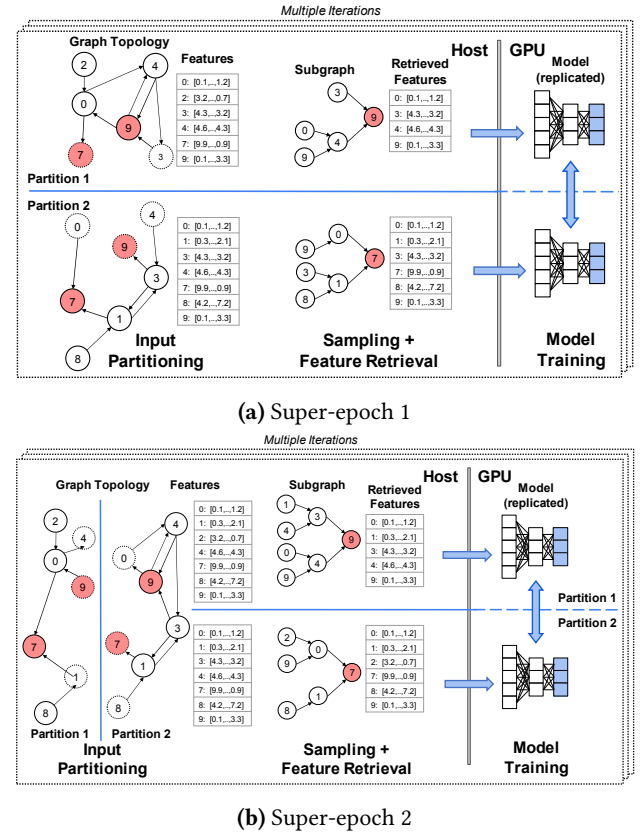


**Figure 2.** Example of GNN training with Grappa for two super-epochs. Compared to Figure 1, subgraph sampling is performed *without remote neighbor fetches* (gradient-only communication) in each iteration and epoch. After a few epochs, we switch to a new super-epoch, creating a new partitioning layout (repartitioning).

consisting of multiple training epochs. The input graph and its features are partitioned at the start of each super-epoch. We keep the partitioning layout unchanged for the entire super-epoch. Training proceeds in epochs that iterate over the whole set of training nodes in steps (also referred to as iterations). Within each step, we construct mini-batches of subgraphs and associated features. The GPU then processes each mini-batch as input for model training. Finally, the gradients are accumulated across all replicated models for each partition before proceeding to the next iteration.

Grappa allows each node to be exposed to its entire neighborhood despite its partition-level isolation by strategically repartitioning the input between super-epochs (§3.3). Repartitioning the input several times throughout the training to disseminate neighborhood information is more cost-effective exchanging data across partitions. The rationale behind this design decision is that, with conventional training, the total neighbor-exchange volume scales roughly with the sum of the fanout at each layer and grows rapidly with model depth and cut edges. In contrast, repartitioning cost is linear in the input size and the number of super-epochs.

Repartitioning alone is insufficient to ensure high model accuracy as, despite exposing each vertex to its entire neighborhood throughout all super-epochs, we may still introduce bias into the sampling process unwillingly. For example, during two super-epochs, a neighbor could be seen more or less frequently due to the partition structure and the presence or absence of an edge. Grappa accounts for sample bias by keeping track of how many times a vertex is seen during a super-epoch and scaling the gradients for that partition before aggregation. We introduce a low-overhead weighted aggregation scheme based on estimations to adjust for sampling bias (§3.4). We directly leverage this scheme in the Grappa training controller to decide when to repartition the graph, switching to the next super-epoch (§3.5).

Intuitively, isolated training is akin to dropout in the input layer, improving generalization for deeper models. Repartitioning restores long-run neighbor coverage, and the coverage-corrected scaling re-centers gradients toward the full-graph objective.

Together, these mechanisms preserve the convergence properties akin to conventional GNN training, enabling the model to effectively learn from the global graph structure while reducing communication overhead.

### 3.2 Isolated Training Strategy

Unlike conventional GNN training systems that typically follow edges to retrieve nodes and features from multiple partitions, Grappa operates entirely within the confines of each local partition, leveraging this isolation to streamline the training process.

**Isolated Training.** Grappa proceeds similarly to traditional training, but considers exclusively local nodes and edges. Since partition creation includes halo<sup>1</sup> nodes that effectively eliminate dependencies on cross-partition edges, Grappa can proceed as if each partition executes message passing on its local subgraph augmented with halos, without remote dependencies within an iteration. In each iteration, we either feed the entire partition to the model (full-graph mode) or select a subset of the training nodes from the local partition to construct subgraphs (sampling mode). Each subgraph's depth aligns with the number of layers in the model, ensuring that every node in the mini-batch has sufficient local neighborhood information.

**Overhead Reduction.** The primary advantage of Grappa's approach is reducing communication overhead and synchronization delays. In traditional GNN training, resource consumption during sampling increases exponentially as the graph size, model depth, and number of partitions increase. By eliminating cross-partition exchange of features or activations during a training iteration, Grappa reduces the time

<sup>1</sup>Halo nodes cache boundary neighbors to complete k-hop neighborhoods within a partition. They are read-only in a super-epoch, contribute to local aggregations, and never trigger cross-partition fetches.

spent on *cross-partition neighbor exchange* to zero, leaving only gradient synchronization. The system still accumulates and updates gradients across partitions after each iteration to ensure the model parameters benefit from each partition. This approach enables both an accelerated training process and enhanced scalability. Isolation introduces a predictable *coverage bias*: a node's gradient in a step reflects only neighbors present in the current partition. We correct this bias in aggregation using a single scalar per batch, derived from easy-to-measure degree ratios (§3.4).

### 3.3 Dynamic Graph Repartitioning

Grappa dynamically manages graph partitions throughout the training process by actively repartitioning the graph to disseminate neighborhood information across the entire graph structure effectively. This dynamic approach contrasts with other GNN training systems that use static partitioning where partitions are not isolated and highlights the importance of adapting the partitioning layout for model quality.

**Super-epochs.** Grappa structures the overall training process into super-epochs. The training controller (§3.5) makes the decision to transition to a new super-epoch where the input graph will undergo repartitioning. The new partitions must be distinct from the partitions in the previous super-epoch to ensure that each vertex is exposed to its entire neighborhood. Once the repartition is complete, we begin executing the next super-epoch. The challenge with repartitioning is that recomputing partitions and shuffling data between each super-epoch may be prohibitively expensive and negate the performance benefits of isolated training.

**Graph Partitioning.** Many graph partitioning strategies exist, such as random or METIS [18]. In random graph partitioning, nodes in the input graph are randomly assigned to different partitions without particular consideration for the underlying graph structure. In contrast, METIS graph partitioning recursively coarsens the graph to reduce its size, partitions the smaller graph, and then uncoarsens it to obtain a balanced and high-quality partition of the original graph. Upon partitioning the nodes, the edges linked to these nodes and their corresponding endpoints are also included in the respective partition. Should an endpoint not be part of the initial partition, it is incorporated as a halo node, represented with dashed lines in Figure 2. Finally, the features associated with each node are added to the partition.

**Chunks and Efficient Partition Construction.** Repartitioning the graph can introduce significant overhead due to the need to assign nodes and edges to a partition and split the associated data, typically floating point vectors of length 128 to 1024 for each node. To mitigate this overhead, Grappa leverages unmodified graph partitioning strategies such as random or METIS to split the dataset into *chunks*, rather than final partitions. This initial partitioning is performed only

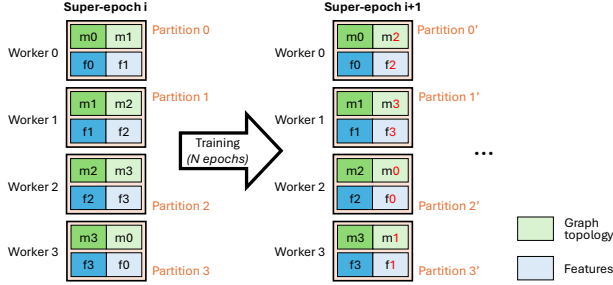


**Figure 3.** Example of efficient dynamic repartitioning via sweeping chunks. The example shows four workers operating in a data-parallel manner. The graph topology and feature data are divided into chunks  $m_0, m_1, m_2, m_3$  and  $f_0, f_1, f_2, f_3$  respectively. The dataset is split into chunks just once before training. The four workers then operate in parallel. Worker 0 initially loads chunks  $m_0$  and  $f_0$ , then loads  $m_1$  and  $f_1$ , groups these together as a partition, and trains the model on the resulting partition for a super-epoch. After that, we perform a repartition where worker 0 will load the next chunks  $m_2$  and  $f_2$ , grouping them with  $m_0, f_0$  to form a new partition for further training. This process repeats until all workers have seen all chunks at least once.

once. Each partition for training is dynamically constructed by combining pairs of chunks, specifically a base chunk,  $m_i$ , with another variable chunk,  $m_j$  where  $i \neq j$ . This approach allows for quick and efficient repartitioning of the graph by sweeping through different variable chunks without recomputing a new set of partitions after each super-epoch. Each worker is responsible one chunk and sweeps one chunk from the other chunks during each repartitioning, thus only loading a small subset of the graph each time. This method effectively disseminates neighborhood information across the graph structure. Figure 3 shows a simple example of Grappa's efficient sweeping chunk partitioning. This coverage holds for  $k$ -layer models as the locality boundary changes across super-epochs, ensuring that neighbors within graph distance  $\leq k$  appear with non-zero probability over time.

**Coverage guarantee.** With  $M + 1$  chunks and  $W$  workers, each worker pins a base chunk  $m_i$  and cycles  $m_j \neq i$  across super-epochs. Over  $M$  super-epochs, every cross-chunk edge co-resides in at least one partition, giving non-zero long-run inclusion probability for all neighbors required by Theorem 3.1. When  $W < M$ , we schedule base chunks in a round-robin tournament so that all pairs  $(m_i, m_j)$  are covered.

The sweep schedule ensures every edge is co-located with its endpoints in multiple super-epochs, which makes the long-run inclusion frequency well-defined and enables consistent bias correction.

### 3.4 Coverage-Corrected Aggregation

**Problem: Local Sampling Bias.** When we train in isolation, a node  $v$  only sees its *local* neighbors in the current partition. The gradient we compute in that step is, therefore, biased toward the local neighborhood. This can be seen as a form of biased sampling and our goal is to correct for it so that model updates reflect the full graph. Our procedure is inspired by [7] but differs in its approach. [7] focus on bias correction in a single layer, while we focus on the gradient. In addition to directly addressing the quantity of interest in training, our approach has the advantage of being model-agnostic, as it does not require modifying activations or other model components but only operates on gradients.

**Solution: Bias-Corrected Estimators.** We propose a set of estimators with different properties that allow tailoring the solution to different use cases. We first propose a node-level estimator that eliminates sampling bias exactly. We then propose a coarser estimator that operates on batch-level gradient objects, enabling compatibility with common software packages [31]. Finally, we propose a shrinkage-based estimator that consciously accepts some bias in order to reduce overfitting.

**Notation.** Consider a model represented by a function  $g_v(u, \theta)$ , parametrized by a parameter vector  $\theta \in \mathbb{R}^{|\theta|}$ , that gives the loss contribution for a node  $v$  of a single neighboring node  $u$ . We omit  $\theta$  for readability. Let  $\mathcal{D}$  be the distribution of nodes in the original graph and  $\mathcal{D}_v$  the conditional distribution of neighbors of  $v$  in the original graph.

**Full-Graph Unbiased Estimator.** The true gradient of the loss function  $L$  is given by:

$$\nabla_\theta L = \mathbb{E}_{v \sim \mathcal{D}} [\mathbb{E}_{u \sim \mathcal{D}_v} [\nabla_\theta g_v(u)]] \quad (1)$$

where the expectation over  $\mathcal{D}_v$  models neighborhood aggregation. This can be estimated by the unbiased estimator:

$$\nabla_\theta \tilde{L} = \frac{1}{|S_{\mathcal{D}}|} \sum_{v \in S_{\mathcal{D}}} \frac{1}{|S_{\mathcal{D}_v}|} \sum_{u \in S_{\mathcal{D}_v}} \nabla_\theta g_v(u) \quad (2)$$

where the samples  $S_{\mathcal{D}}$  and  $S_{\mathcal{D}_v}$  are i.i.d. draws according to the original distributions  $\mathcal{D}$  and  $\mathcal{D}_v$ .

**Sampling Bias in Isolated Training.** Viewed across partitions, nodes are still sampled from the full distribution  $\mathcal{D}$  in the isolated training strategy. Neighboring nodes, however, are drawn from the conditional distribution  $\mathcal{D}_v^{\text{local}}$  of neighboring nodes of  $v$  present in the local partition.

**Importance Weighting.** We want to re-weight gradient contributions to recover the true gradient  $\nabla_\theta L$  (1). Our guiding idea will be a well-known importance sampling result [11] that allows recovering the original distribution. Denoting the probabilities of selecting a neighboring node  $u$

under the original distribution  $\mathcal{D}_v$  and under the local distribution  $\mathcal{D}_v^{\text{local}}$  by  $p_v(u)$  and  $q_v(u)$ , respectively, we have:

$$\begin{aligned} \mathbb{E}_{v \sim \mathcal{D}} \left[ \mathbb{E}_{u \sim \mathcal{D}_v^{\text{local}}} \left[ \frac{p_v(u)}{q_v(u)} \nabla_{\theta} g_v(u) \right] \right] &= \\ \mathbb{E}_{v \sim \mathcal{D}} \left[ \mathbb{E}_{u \sim \mathcal{D}_v} [\nabla_{\theta} g_v(u)] \right] &= \nabla_{\theta} L \end{aligned} \quad (3)$$

if  $q_v(u) > 0$  whenever  $p_v(u) > 0$ .

**Asymptotically Unbiased Node-Level Estimator.** We cannot apply the importance sampling result (3) directly because the probability of selecting a neighbor missing from the local partition is zero, violating the support condition. We resolve this via repartitioning: as long as the long-run probability is positive, the bias can be removed entirely, at least asymptotically. The sweep schedule presented in §3.3 guarantees that each node will be matched with all of its neighbors already after a finite number of super-epochs, so the assumption is justified. Formally, let  $q_v^t(u) = \mathbb{P}[u \in S_{\mathcal{D}_v^{\text{local}}}^t]$  be the probability of selecting neighbor  $u$  of  $v$  in the current local partition at super-epoch  $t$ . We define the estimator:

$$\begin{aligned} \nabla_{\theta} \tilde{L}^{\text{corr}} &= \\ \frac{1}{T} \sum_{t=1}^T \frac{1}{|S_{\mathcal{D}}^t|} \sum_{v \in S_{\mathcal{D}}^t} \frac{1}{|S_{\mathcal{D}_v^{\text{local}}}^t|} \sum_{u \in S_{\mathcal{D}_v^{\text{local}}}^t} \frac{p_v(u)}{q_v^t(u)} \nabla_{\theta} g_v(u) & \end{aligned} \quad (4)$$

where  $T$  is the number of super-epochs and  $|S_{\mathcal{D}}^t|$  is the local node sample in the current super-epoch. If the partitioning gives enough weight to each node such that:

$$\lim_{T \rightarrow \infty} \frac{1}{T} \sum_{t=1}^T \mathbb{E}_{u \in S_{\mathcal{D}_v^{\text{local}}}^t} q_v(u) \xrightarrow{\text{a.s.}} q_v(u) > 0 \quad (5)$$

i.e., the long-run selection probability is positive, we have:

**Theorem 3.1.** *Under assumption (5) and if  $\left| \frac{p_v(u)}{q_v^t(u)} \nabla_{\theta} g_v(u) \right| \leq M$  for some constant  $M$  and  $S_{\mathcal{D}}^t$  and  $S_{\mathcal{D}_v^{\text{local}}}$  are i.i.d. samples,*

$$\lim_{T \rightarrow \infty} \mathbb{E} [\nabla_{\theta} \tilde{L}^{\text{corr}}] = \nabla_{\theta} L \quad (6)$$

i.e.,  $\nabla_{\theta} \tilde{L}^{\text{corr}}$  is asymptotically unbiased under mild regularity conditions. An important special case is when all neighbors have equal weight under  $\mathcal{D}_v$  for all  $v$ . Then  $p_v(u) = 1/d_v^{\text{global}}$ ,  $q_v^t(u) = 1/d_v^{\text{local}}$  for all local neighbors  $u$  of  $v$ , where  $d_v^{\text{global}}$  and  $d_v^{\text{local}}$  are the degrees of node  $v$  in the full graph and in the local partition, respectively. So  $\nabla_{\theta} \tilde{L}^{\text{corr}}$  becomes:

$$\begin{aligned} \nabla_{\theta} \tilde{L}^{\text{uniform}} &= \\ \frac{1}{T} \sum_{t=1}^T \frac{1}{|S_{\mathcal{D}}^t|} \sum_{v \in S_{\mathcal{D}}^t} \frac{1}{|S_{\mathcal{D}_v^{\text{local}}}^t|} \frac{d_v^{\text{local}}}{d_v^{\text{global}}} \sum_{u \in S_{\mathcal{D}_v^{\text{local}}}^t} \nabla_{\theta} g_v(u) & \end{aligned} \quad (7)$$

In general one may use  $q_v^t(u) = p_v(u) / \sum_{i \in \mathcal{D}_v^{\text{local}}} p_v(i)$ .

**Batch-Level Approximation.** Exact bias correction requires modifying gradient contributions at the level of individual nodes in a batch. Common libraries such as PyTorch

[31] only provide hooks for modifying batch-level gradient objects, however. In line with the idea of being model-agnostic, it would be desirable to have a framework that can be used with [31] and its batch-level gradient objects. We propose the following batch-level estimator and will proceed to show that it is closest (in L2-distance of expectations) to the asymptotically unbiased estimator under mild assumptions:

$$\begin{aligned} \nabla_{\theta} \tilde{L}^{\text{batch}}(c) &= \\ \frac{1}{T} \sum_{t=1}^T \frac{c^t}{|S_{\mathcal{D}}^t|} \sum_{v \in S_{\mathcal{D}}^t} \frac{1}{|S_{\mathcal{D}_v^{\text{local}}}^t|} \sum_{u \in S_{\mathcal{D}_v^{\text{local}}}^t} \nabla_{\theta} g_v(u) & \end{aligned} \quad (8)$$

where the batch-level correction factors  $c \in \mathbb{R}^T$  are:

$$c^t = \frac{1}{|S_{\mathcal{D}}^t|} \sum_{v \in S_{\mathcal{D}}^t} \frac{1}{|S_{\mathcal{D}_v^{\text{local}}}^t|} \sum_{u \in S_{\mathcal{D}_v^{\text{local}}}^t} \frac{p_v(u)}{q_v^t(u)} \quad (9)$$

In the case of equal selection probabilities, this simplifies to:

$$c_{\text{uniform}}^t = \frac{1}{|S_{\mathcal{D}}^t|} \sum_{v \in S_{\mathcal{D}}^t} \frac{d_v^{\text{local}}}{d_v^{\text{global}}} \quad (10)$$

In practice, we apply the batch-level correction  $\nabla_{\theta} \tilde{L}^{\text{batch}}(c)$  before the phase's gradient synchronization. We have (for notational convenience, we set  $T = 1$  without loss of generality and drop the  $t$ -superscript):

**Theorem 3.2.** *Assuming that gradients are independently identically distributed  $\nabla_{\theta} g_v(u) \sim \text{i.i.d}$  with finite mean  $\mu \in \mathbb{R}^{|\theta|} \setminus \mathbf{0}$  independent of  $\frac{p_v(u)}{q_v(u)}$ , equation (9) gives the scalar  $c$  that minimizes:*

$$\left\| \mathbb{E} [\nabla_{\theta} \tilde{L}^{\text{corr}}] - c \mathbb{E} [\nabla_{\theta} g_{S_{\mathcal{D}}}] \right\|_2 \quad (11)$$

i.e.,  $\nabla_{\theta} \tilde{L}^{\text{batch}}$  is the estimator with batch-level correction whose expectation is closest (in  $L^2$ -distance) to the expectation of  $\nabla_{\theta} \tilde{L}^{\text{corr}}$  under mild distributional assumptions.

**Shrinkage.** Above, we have derived asymptotically unbiased and minimally-biased estimators under idealized assumptions. In practice, accepting some degree of bias to shrink coefficients can improve stability and combat overfitting [15]. We find that the following correction factor gives better accuracy than the minimally-biased version:

$$c_{\text{resampling}}^t = \frac{1}{\sum_{v \in S_{\mathcal{D}}^t} \left[ \frac{d_v^{\text{global}}}{d_v^{\text{local}}} - 1 \right] |S_{\mathcal{D}_v^{\text{local}}}^t|} \quad (12)$$

While  $c^t$  uses an arithmetic mean of correction factors,  $c_{\text{resampling}}^t$  is closer to a harmonic mean and produces lower correction factors overall. We interpret this as a form of shrinkage in gradient magnitude, similar to methods like gradient clipping and others that have been developed for deep learning applications [30, 32]. Intuitively,  $c_{\text{resampling}}^t$  weights the correction factors inversely by how often, in expectation, the global set of neighbors of a selected node would have to be resampled to get a sample consisting only of neighbors present in the local partition.

### 3.5 Training Controller and Partitions Switching

The training process in Grappa is managed and monitored by a training controller that collects information on the overall training progress on each machine and for each partition. The controller aggregates sampling information within each partition and initiates repartitioning when appropriate.

The controller currently aims to ensure that each possible combination of chunks for a partition are explored for a fixed number of iterations, providing it with a target of  $e/(c-1)$  super-epochs where  $e$  is a fixed number of epochs to train for and  $c$  is the number of chunks in the system. The controller monitors a simple *coverage deficit* statistic per partition,  $\Delta_t = 1 - \hat{c}_t$ , and triggers an earlier repartitioning when  $\Delta_t$  persists across several steps, prioritizing partitions with low coverage. Gradient aggregation is performed synchronously within the current phase; repartitioning only updates metadata and does not introduce neighbor traffic. We empirically verify that this simple heuristic is sufficient for our needs (§5). Therefore, we leave the implementation of more sophisticated switching heuristics for future work.

### 3.6 Phase-Parallel Training

Grappa's isolated training approach substantially increases the flexibility of parallel training. Since training is performed in isolation for each partition with no cross-partition communication or synchronization, Grappa allows for an unconventional yet highly effective training method: the sequential execution of multiple partitions in phases. This strategy significantly amplifies training capacity, which benefits large input graphs that do not fit into the collective memory of all available machines.

When accommodating concurrent training on all partitions is unfeasible, Grappa can adopt a phase-parallel training approach that divides the partitions into distinct phases, each involving the execution of only a subset of the total partitions. However, this approach introduces an essential change in handling gradient aggregation: exchanging and aggregating gradients across all partitions becomes impractical. Instead, we synchronize gradients among only the partitions involved in a specific training phase.

Algorithm 1 shows the phase-parallel training process in Grappa. The algorithm depends on  $P$ , the number of partitions, and  $M$ , the number of partitions per phase. By default, Grappa trains with  $P = M$ , but it can train with  $M < P$  as well. In particular,  $M = 1$  allows the system to train on an arbitrarily large graph using a single machine.

Grappa's phase-parallel training enables trading off training time for capacity.

## 4 Implementation

Grappa follows a client-server architecture that enforces gradient-only communication. Servers store the graph structure and node features while clients issue sampling requests

---

### Algorithm 1: Phase Parallel Training in Grappa

---

**Input:** Graph  $G$ , number of partitions  $P$ , max partitions per phase  $M$   
**Output:** Trained model parameters

- 1 Initialize model parameters;
- 2 Partition  $G$  into  $P$  partitions;
- 3 **for** each epoch **do**
- 4     **for**  $i \leftarrow 1$  to  $\lceil P/M \rceil$  **do**
- 5         Let partitions be the partitions for phase  $i$ ;
- 6         gradients  $\leftarrow []$ ;
- 7         **for** each partition in partitions **do in parallel**
- 8             sampled  $\leftarrow$  isolated\_sampling(partition);
- 9             outputs  $\leftarrow$  forward\_pass(sampled);
- 10             gradient  $\leftarrow$  compute\_gradients(outputs);
- 11             gradients.append(gradient);
- 12         agg\_gradient  $\leftarrow \frac{1}{|gradients|} \sum_{g \in gradients} g$ ;
- 13         Update model using agg\_gradient;
- 14 **return** model

---

and drive training. During training, servers never exchange features or activations across partitions. Cross-server traffic consists only of gradient all-reduce and occasional repartitioning metadata at super-epoch boundaries.

We run one server and one client per partition, co-located on the same machine for locality. Each client samples subgraphs from its local partition on the CPU and feeds batches to the GPU for forward and backward passes. Gradients are computed locally and then aggregated across the concurrently active partitions to update model parameters. This preserves the per-iteration invariant of gradient-only communication while supporting both fully parallel and phase-parallel execution.

**Estimator choice.** We use batch-level coverage-corrected aggregation  $\nabla_{\theta} \tilde{L}^{\text{batch}}(c)$  (Eq. (8)) with the resampling-based factor  $c_{\text{resampling}}^t$  (Eq. (12)). This design integrates cleanly with PyTorch as a single per-batch gradient scaling hook (applied immediately before the all-reduce), adds negligible overhead, and avoids re-implementing node-level gradient accounting. The node-level variant would require substantial custom machinery in PyTorch, complicating fair performance comparisons against highly optimized baselines. The results for the minimally biased variant are shown in Appendix C.

We build Grappa on top of Deep Graph Library (DGL) [43] and use PyTorch [31] for model execution. DGL provides efficient sampling and partitioned data access on single machines and clusters; Grappa layers gradient-only communication, repartitioning, and batch-level correction on top.

## 5 Evaluation

In this section, we conduct a comprehensive evaluation of Grappa through a multifaceted approach that includes end-to-end benchmarks and microbenchmarks. Our primary emphasis is on model-level metrics (train accuracy, test accuracy) and system-level metrics (throughput, runtime, capacity). We focus on providing in-depth answers to the following research questions.

**RQ1:** How does the performance of Grappa compare to state-of-the-art distributed training systems in terms of training time and accuracy? (§5.2)

**RQ2:** How does Grappa scale as the number of graph partitions or the graph size increases? In particular, can phase-parallel training enable the training of very large graphs that do not fit in a single machine? (§5.3)

**RQ3:** What are the overheads and benefits of the various components of Grappa? (§5.4)

### 5.1 Experimental Setup

**GNN Models.** We use three standard GNN models for our experiments, illustrating a varied set of graph-based tasks.

**GraphSage (Sage)** [13] is a general inductive framework that efficiently generates low-dimensional node embeddings for previously unseen data. At each layer, the hidden states of a node's neighbors are first aggregated (for example, by averaging). These states and the states from the previous layer are combined and multiplied by a matrix. This process yields the hidden state at the current layer.

**Graph Convolutional Network (GCN)** [20] is one semi-supervised technique used for classifying nodes within graph-structured data. In each layer, the hidden states (or the initial features) are multiplied by a matrix, functioning as a linear layer. Then, a node's final hidden states at this layer are obtained by averaging the hidden states of all its neighbors, weighted by using their degrees.

**Graph Attention Network (GAT)** [40] assigns weights to different neighborhood nodes using attention. This approach makes aggregating neighborhood information more adaptable. In each layer, the hidden states (or features at the beginning) are modified by a matrix (a linear layer). The final hidden states of a node are determined by averaging its neighbors' hidden states using learned weights.

In this evaluation, we refer to a model with  $k$  layers by appending the layers to the model's abbreviated name, e.g., a three-layer GraphSage model is referred to as Sage-3.

**Datasets.** We use the datasets shown in Table 2, representing a diverse range of graph sizes and characteristics.

In addition to these real-world datasets, we use synthetic graphs based on the Graph500 RMAT generator [29] in scalability experiments. RMAT graphs support different scales, denoted RMAT-X, corresponding to a synthetic graph with  $2^X$  nodes following a power-law degree distribution with an average degree of 16. We use a feature dimension of

Name	Dataset	Vertices	Edges	Features
OGBN-Ar	OGBN ArXiv [2]	0.16M	1.11M	128
Reddit	Reddit [1]	0.22M	109.30M	602
OGBN-Pr	OGBN Products [3]	2.34M	58.99M	100
OGBN-Pa	OGBN Papers100M [4]	105.92M	1.51B	128
RMAT-X	RMAT Scale X [29]	$2^X$	$2^{X+4}$	128

**Table 2.** Datasets used in the experiments.

128 for all RMAT graphs. RMAT-26 contains approximately  $2^{30} \approx 1.07$  billion edges; RMAT-30 contains approximately  $2^{34} \approx 17.18$  billion; RMAT-36 contains approximately  $2^{40} \approx 1.10$  trillion. We use the official graph splits where available.

**Baselines.** We compare Grappa against three carefully selected baselines: DGL [43], MGG [45], and Cluster-GCN [8]. These baselines represent a broad spectrum of GNN systems, covering both distributed and single-node settings and different training paradigms (full-graph and sampling).

**DGL** is a widely used distributed GNN training framework that supports both full-graph and sampling-based training. It is the closest state-of-the-art system to Grappa, as both systems utilize CPUs for sampling and GPUs for forward and backward computation. DGL provides a direct comparison with an established distributed GNN system.

**MGG** is a recent, high-performance full-graph system optimized for multi-GPU training on a single node. It leverages fast NVLink bandwidth between GPUs but does not support distributed execution. We include MGG as it represents the best-in-class single-node full-graph training system, providing a valuable contrast to Grappa's distributed design.

**Cluster-GCN** offers a fundamentally different approach to sampling-based training by leveraging graph clustering to precompute training batches (clusters). This method eliminates the need for expensive runtime sampling or communication overhead, achieving similar goals to Grappa but through a different approach. However, Cluster-GCN is specialized for GCN models and does not generalize to other GNN architectures. Its inclusion in our baselines highlights the trade-offs between specialization and generality in GNN training systems.

**Hardware and Configuration.** We use two different systems for the evaluation. We evaluate distributed training systems on a cluster of 8 identical machines. Each machine is equipped with 2 Intel CPUs (Xeon Gold 6134M), 764 GB of DDR4 memory, and two Nvidia Tesla V100 PCIe 32 GB GPUs. These machines are connected by  $2 \times 10$  Gb/s network (joined as one bonding interface). For single node evaluation, we also use a machine with 2 AMD CPUs (EPYC 9654), 2 TB of DDR5, and 8 Nvidia Hopper H100 80 GB SXM GPUs that are fully connected with 900 GB/s NVLink. The operating system is a 64-bit Debian Linux (kernel version: 5.15); we use CUDA 11.8 and run all experiments in docker containers.

We strive to ensure comparable and fair results across all systems in each experiment. We maintain consistency by

using the same batch size (1000) for all mini-batch training systems. We set the number of sampled neighbors at each layer to {25,10}, {15,10,5}, and {20,15,10,5} for models with 2, 3, and 4 layers, respectively. Moreover, we standardize key hyperparameters: a hidden dimension of 128, a learning rate of 0.003, a dropout rate of 0.5, and a training duration of 500 epochs are applied uniformly. We use the batch-level version of Grappa’s gradient correction  $\nabla_{\theta} \tilde{L}^{\text{batch}}(c)$  (8) with resampling-based correction factors  $c_{\text{resampling}}^t$  (12). We also conducted hyperparameter sensitivity experiments that showed almost no discernible differences in performance across different configurations when comparing the systems, indicating that our chosen settings are representative and fair. Finally, we make a concerted effort to optimally configure all systems under comparison and run each experiment multiple times to ensure statistically significant results.

## 5.2 Training Efficiency and Accuracy (RQ1)

We first assess the overall performance of Grappa by comparing it with our baselines.

**5.2.1 Epoch Time.** We start with a broad comparison of epoch time between Grappa and DGL for combinations of datasets in Table 2 and models (§5.1) with several layers ranging from 2 to 4. We partition each dataset into 16 partitions executing in a different GPU for a total of 16 GPUs. Table 3 presents the results of this experiment.

The average epoch time differs across models and datasets. DGL-Metis is faster than DGL-Random because it reduces cross-partition neighbor traffic through fewer edge cuts, though at the cost of expensive upfront partitioning that can require as much memory as training itself. In contrast, Grappa avoids cross-partition feature and activation exchange within an iteration (requiring only gradient communication), leading to 1×–13× speedups over DGL (4× on average). In summary, Grappa cuts training time by up to an order of magnitude compared to DGL.

**5.2.2 Accuracy.** Grappa outperforms DGL-Random and DGL-Metis, achieving an average accuracy of 68% across the tested scenarios, compared to 61% for both DGL systems. Table 4 shows that this difference is mainly explained by Grappa’s increasingly better accuracy for deeper models. DGL and Grappa have comparable accuracy for 2-layer models, all at 69%, but accuracy drops sharply for both DGL systems to around 63% and 51% for 3- and 4-layer models, respectively, while Grappa’s accuracy stays relatively flat around 67%. We speculate that this is due to the dropout-like nature of Grappa’s isolated training, where input nodes are removed at random, hence avoiding overfitting and improving generalization. Convergence behavior is similar to DGL and discussed in Appendix D.

	2-layer	3-layer	4-layer	Overall
<b>DGL-Random</b>	0.6894	0.6326	0.5145	0.6122
<b>DGL-Metis</b>	0.6909	0.6328	0.5045	0.6094
<b>Grappa</b>	0.6894	0.6746	0.6664	0.6768

Table 4. Average test accuracy across model depths.

In summary, Grappa achieves comparable or better training accuracy than other state-of-the-art GNN training systems, with the gap widening as models get deeper.

**5.2.3 Sampling Overhead.** We compare Grappa and Cluster-GCN, a sampling-based GNN training system that presents a low-communication alternative design. Cluster-GCN pre-computes training batches via graph clustering, thereby eliminating the need for on-the-fly sampling and reducing communication overhead across partitions. Table 5 shows the average epoch time and test accuracy on GCN-2 for OGBN-Pr.

Although Cluster-GCN achieves an epoch time of around half that of Grappa, Grappa consistently achieves better model accuracy. Moreover, creating the clusters for OGBN-Pr takes 881 seconds for this dataset. In comparison, Grappa’s total overhead for this experiment amounts to 49 (partitioning) + 76 (all super-epoch switches) = 125 seconds. If we consider a generous 500-epoch training run, the total time for Cluster-GCN is 1481 seconds, whereas Grappa requires a total time of 1425. Finally, it is noteworthy that Cluster-GCN is designed explicitly for GCNs and does not extend its benefits to other GNN architectures. Cluster-GCN also eliminates most neighbor traffic via precomputed clusters whereas our approach eliminates it during iterations and retains generality across GNN architectures. In summary, specialized methods like Cluster-GCN underscore the benefits of pre-processing to reduce communication overhead that achieves similar runtime benefits as Grappa but cannot support broader applications.

**5.2.4 Full-Graph Training Time.** Finally, we compare Grappa with MGG, a high-performance full-graph training system optimized for multi-GPU setups on a single node. MGG utilizes NVLink bandwidth for efficient training but does not support distributed execution. Table 6 shows the average epoch time for training a GCN-2 model across various datasets and GPU configurations for both systems. Note that, in this experiment, Grappa runs in full-graph training mode.

As a best-in-class GNN training system, MGG achieves subsecond epoch time on small datasets (OGBN-Pr and Reddit) and 2.1-second for the larger OGBN-Pa, faster than similar systems such as BNS-GCN [42] and NeutronStar [44]. Since it must store the entire graph on HBM, MGG runs out of memory to process OGBN-Pa with only 2 and 4 GPUs. In comparison, Grappa does not suffer from the same memory capacity limitation and achieves faster full-graph epoch times since it incurs zero communication overhead.

Model	Systems	Average epoch time				Test accuracy			
		OGBN-Ar	Reddit	OGBN-Pr	OGBN-Pa	OGBN-Ar	Reddit	OGBN-Pr	OGBN-Pa
<b>Sage-2</b>	DGL-Random	0.6 s	6.2 s	4.2 s	15.5 s	0.5630	0.9626	0.7748	0.4877
<b>Sage-2</b>	DGL-Metis	0.4 s	3.7 s	2.3 s	9.1 s	0.5649	0.9633	0.7756	0.4866
<b>Sage-2</b>	Grappa	0.4 s	1.0 s	1.3 s	3.9 s	0.5571	0.9633	0.7688	0.4676
<b>GCN-2</b>	DGL-Random	0.6 s	6.2 s	4.2 s	15.0 s	0.5078	0.9211	0.7651	0.4734
<b>GCN-2</b>	DGL-Metis	0.4 s	3.7 s	2.3 s	9.1 s	0.5055	0.9209	0.7676	0.4761
<b>GCN-2</b>	Grappa	0.4 s	1.0 s	1.3 s	3.8 s	0.5416	0.9472	0.7663	0.4886
<b>GAT-2</b>	DGL-Random	0.7 s	6.3 s	4.4 s	14.9 s	0.5682	0.9493	0.7881	0.5115
<b>GAT-2</b>	DGL-Metis	0.5 s	3.8 s	2.4 s	9.9 s	0.5741	0.9525	0.7902	0.5130
<b>GAT-2</b>	Grappa	0.4 s	1.1 s	1.4 s	5.1 s	0.5430	0.9476	0.7829	0.4984
<b>Sage-3</b>	DGL-Random	0.9 s	9.7 s	8.5 s	22.9 s	0.5553	0.9593	0.7513	0.4435
<b>Sage-3</b>	DGL-Metis	0.6 s	6.2 s	4.5 s	16.1 s	0.5567	0.9635	0.7527	0.4489
<b>Sage-3</b>	Grappa	0.4 s	1.0 s	1.4 s	4.9 s	0.5532	0.9589	0.7738	0.4259
<b>GCN-3</b>	DGL-Random	0.9 s	9.8 s	8.5 s	23.2 s	0.4984	0.6527	0.6132	0.4355
<b>GCN-3</b>	DGL-Metis	0.6 s	6.0 s	4.5 s	16.1 s	0.4857	0.6593	0.6164	0.4384
<b>GCN-3</b>	Grappa	0.4 s	1.0 s	1.4 s	4.8 s	0.5172	0.9326	0.7502	0.4333
<b>GAT-3</b>	DGL-Random	1.0 s	10.0 s	9.0 s	23.7 s	0.5688	0.8999	0.7160	0.4971
<b>GAT-3</b>	DGL-Metis	0.7 s	6.4 s	5.1 s	20.4 s	0.5755	0.8650	0.7182	0.5130
<b>GAT-3</b>	Grappa	0.5 s	1.1 s	1.6 s	5.8 s	0.5487	0.9251	0.7855	0.4902
<b>Sage-4</b>	DGL-Random	1.5 s	16.6 s	40.2 s	54.2 s	0.5237	0.9514	0.6692	0.4237
<b>Sage-4</b>	DGL-Metis	1.0 s	13.1 s	20.0 s	39.2 s	0.5285	0.9486	0.6718	0.4297
<b>Sage-4</b>	Grappa	0.4 s	1.3 s	1.5 s	5.7 s	0.5428	0.9633	0.7946	0.4174
<b>GCN-4</b>	DGL-Random	1.5 s	16.7 s	40.1 s	53.8 s	0.5121	0.2540	0.2658	0.4113
<b>GCN-4</b>	DGL-Metis	1.0 s	13.1 s	20.0 s	39.4 s	0.5203	0.1091	0.2737	0.4204
<b>GCN-4</b>	Grappa	0.4 s	1.3 s	2.5 s	5.7 s	0.5190	0.9180	0.7124	0.4203
<b>GAT-4</b>	DGL-Random	1.7 s	18.0 s	55.6 s	69.0 s	0.5619	0.6755	0.4423	0.4833
<b>GAT-4</b>	DGL-Metis	1.1 s	14.0 s	22.3 s	43.9 s	0.5735	0.6476	0.4430	0.4876
<b>GAT-4</b>	Grappa	0.5 s	1.5 s	3.2 s	7.6 s	0.5249	0.9141	0.7784	0.4914

**Table 3.** Average epoch time and test accuracy across all systems, models, model configurations, and datasets. Datasets are partitioned into 16 partitions and run in 16 GPUs. We run this experiment on our 8-machine V100 cluster.

System	Epoch time	Test accuracy
<b>Cluster-GCN</b>	1.2 s	0.7390
<b>Grappa</b>	2.6 s	0.7663

**Table 5.** Average epoch time and test accuracy of Cluster-GCN and Grappa on GCN-2 for OGBN-Pr. Experiment run on our H100 machine.

Even if MGG were to support multi-node execution, it would necessitate expensive communication links and would still be constrained by the requirement to store the entire graph on the GPUs. This limitation highlights the advantages of Grappa's distributed architecture, which can efficiently manage larger datasets across multiple nodes without the same memory constraints.

In summary, Grappa's flexible and isolated training design outperforms single-node systems like MGG and does not suffer from the same communication bottleneck.

### 5.3 Scalability and Capacity (RQ2)

We now evaluate the scalability of Grappa as we increase the number of partitions and the graph size. We also show

Dataset	Method	2 GPU	4 GPU	8 GPU
Reddit	<b>MGG</b>	0.2 s	0.2 s	0.2 s
	<b>Grappa</b>	0.4 s	0.2 s	0.1 s
OGBN-Pr	<b>MGG</b>	0.3 s	0.2 s	0.2 s
	<b>Grappa</b>	0.4 s	0.2 s	0.1 s
OGBN-Pa	<b>MGG</b>	Crash	Crash	2.8 s
	<b>Grappa</b>	5.7 s	3.5 s	2.4 s

**Table 6.** Average epoch time for MGG and Grappa (full-graph training mode) to train a GCN-2 model for different datasets and across different GPU configurations. Experiment run on a machine with 8×H100 with full NVLink connections.

how Grappa's phase-parallel training allows the system to train very large graphs using limited resources.

**5.3.1 Increasing Number of Partitions.** We measure the average epoch time using Sage-3 and the different datasets in Table 2 as we increase the number of partitions from 1 to 64. Figure 4 shows the training time per epoch for Grappa

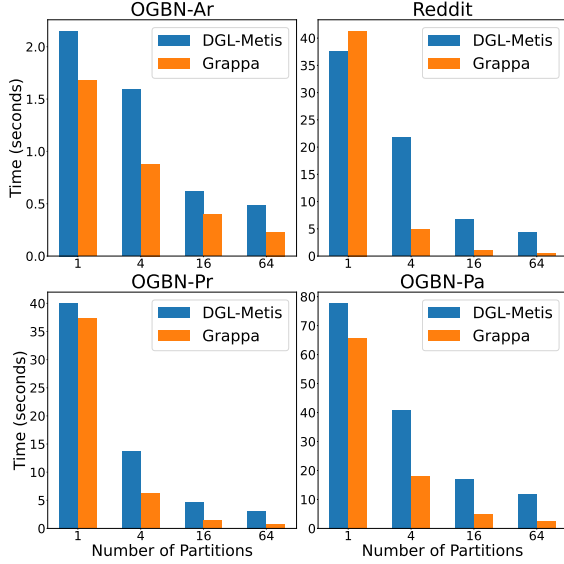


**Figure 4.** Epoch time versus partitions for Sage-3 using Grappa and DGL (one partition per GPU). For Grappa, cross-partition communication is gradient-only and neighbor traffic is zero. Cluster: 8×V100.

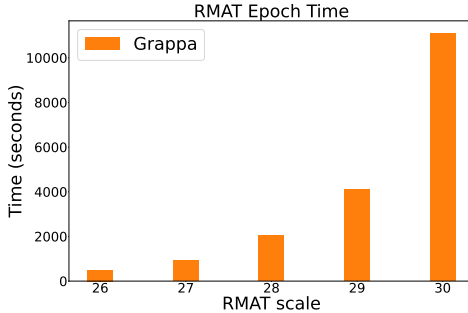


**Figure 5.** Epoch time for Sage-3 with 16 partitions as RMAT size scales (26→30). Grappa uses gradient-only communication (no neighbor traffic). 8×V100 cluster.

and the DGL baseline with METIS partitioning as we vary the number of partitions.

DGL scales poorly compared to Grappa as partitions increase, despite high-quality METIS cuts. For instance, from 1 to 16 partitions, DGL achieves only  $\sim 3\text{--}5\times$  speedup instead of the ideal  $16\times$ , due to growing sampling communication overheads. In contrast, Grappa scales almost linearly ( $\sim 16\times$ ) on all datasets except OGBN-Ar, whose small, highly connected graph amplifies system overheads relative to epoch time. In summary, Grappa’s training time scales nearly linearly with partition count.

**5.3.2 Increasing Graph Size.** We now evaluate Grappa’s performance as we increase the graph size while keeping a fixed number of 16 partitions. To that end, we train Sage-3 on RMAT [29] synthetic graphs and generate random vertex features, doubling the graph size from RMAT-26 to RMAT-30 each time. Figure 5 shows the results of this experiment.

As with the previous experiment, by sampling each partition in isolation, Grappa remains largely unaffected by the graph size and scales almost linearly. In summary, Grappa’s training time scales almost linearly with the graph size.

**5.3.3 Training Very Large Graphs.** Finally, we demonstrate Grappa’s ability to train GNNs on very large graphs that do not fit on a single machine. We use Sage-3 and RMAT-36, partition it into 256 partitions, and train one partition at a time using our phase-parallel approach (§3.6). We find that Grappa can run one epoch of Sage-3 on RMAT-36 in 3.6 hours on a single V100 machine. While training such a model to converge would take a long time, these results show that it can be done on a single machine if needed. This result demonstrates the feasibility of processing trillion-edge topologies on a single machine in phase-parallel mode with gradient-only communication, under a realistic memory budget.

#### 5.4 Ablation Study and Overheads (RQ3)

Finally, we conduct an ablation study to quantify the contribution of each component and the overheads of Grappa.

**5.4.1 Ablation Study.** We conduct an ablation study to assess the contribution of each component of Grappa by comparing it with three variants: *Grappa-UW*, without coverage-corrected aggregation; *Grappa-FP*, with fixed (non-switchable) partitions; and *Grappa-50S*, which relaxes isolation by sampling 50% of vertices from remote partitions. Table 7 presents the results of this experiment.

	GCN-3	Sage-3	GAT-3
<b>Grappa</b>	0.9326	0.9589	0.9251
<b>Grappa-UW</b>	0.8284	0.9636	0.8403
<b>Grappa-FP</b>	0.8464	0.9556	0.9068
<b>Grappa-50S</b>	0.6593	0.9635	0.8999

**Table 7.** Ablation study. We train each of our 3-layer models on the Reddit dataset with a fixed number of 16 partitions on our 8-machine V100 cluster for up to 500 epochs and report the test accuracy.

As expected, both *Grappa-UW* and *Grappa-FP* show lower accuracy than Grappa, showing that coverage-corrected gradient aggregation and repartitioning are important success factors. Interestingly, even *Grappa-50S* has lower accuracy than Grappa, but higher than *Grappa-UW* and *Grappa-FP*, despite having better access to the full graph. This shows that isolated training, when coupled with coverage-corrected gradient aggregation and repartitioning, can outperform full-graph training thanks to its dropout-like nature. This is in addition to the benefit of reduced training time.

In summary, each of Grappa’s key components contributes to ensuring the highest possible model quality.

**5.4.2 Overheads.** Grappa's design introduces three kinds of overheads: partitioning, switching partitions, and redundant storage of a subset of vertices. This section analyzes each of these sources of overhead individually.

Table 8 shows the time taken by Grappa to create 4, 16, and 64 partitions of the OGBN-Pa dataset.

	4 parts.	16 parts.	64 parts.
<b>Grappa</b>	2,110 s	2,568 s	2,345 s
<b>DGL METIS</b>	6,262 s	6,523 s	7,292 s

**Table 8.** Partitioning time for Grappa and DGL on the OGBN-Pa data for different numbers of partitions. Experiment run on our 8-machine V100 cluster.

The partitioning time remains relatively stable despite the increasing number of partitions as Grappa's default partitioning scheme is based on random graph partitioning. The system does not require sophisticated partitions, e.g., using algorithms such as METIS, to achieve fast training time with high testing accuracy. In comparison, DGL with METIS partitioning requires almost 2 $\times$  to 5 $\times$  more time to partition the same dataset using METIS. In summary, Grappa's partitioning overhead is lower than more sophisticated alternatives.

Table 9 shows the overhead of switching partitions during a Sage-3 model training on OGBN-Pr. We include the total training time, the time spent switching partitions, and the fraction of the training time that partitions switching corresponds to for 4, 16, and 64 partitions.

	4 parts.	16 parts.	64 parts.
<b>Training time</b>	3,100 s	700 s	375 s
<b>Switching time</b>	128 s	76 s	51 s
<b>Overhead</b>	4%	10%	12%

**Table 9.** Repartition overhead. Time spent training and switching partitions (repartitioning) while training a Sage-3 model on OGBN-Pr. Cluster: 8 $\times$ V100.

In all cases, the switching time introduces low overhead, i.e., a small fraction of the training time is required for repartitioning to ensure a high model quality. This overhead pales compared to the speedups enabled by isolated training, e.g., over 6 $\times$  in this case. In summary, Grappa's repartitioning overhead is at most 12% of the training time for 64 partitions.

Finally, Table 10 shows the size of each partition and the total size of all partitions using Grappa's partitioning. We fix the number of partitions to 4 and show the results in Table 2.

Random partitioning balances partitions well, with a slight size increase. METIS yields smaller, potentially imbalanced partitions. Grappa efficiently handles both, maintaining high accuracy through repartitioning and coverage-corrected aggregation. In summary, Grappa's partitioning scheme is balanced and memory efficient.

Dataset	Part. 1	Part. 2	Part. 3	Part. 4	Total
<b>Grappa's Random Partitioning</b>					
<b>OGBN-Ar</b>	0.08	0.08	0.08	0.08	0.11
<b>Reddit</b>	1.37	1.38	1.38	1.37	2.27
<b>OGBN-Pr</b>	1.83	1.83	1.83	1.83	2.86
<b>OGBN-Pa</b>	56.70	56.68	56.68	56.69	78.69

Dataset	Part. 1	Part. 2	Part. 3	Part. 4	Total
<b>DGL's METIS Partitioning</b>					
<b>OGBN-Ar</b>	0.06	0.06	0.06	0.06	0.11
<b>Reddit</b>	1.54	1.40	1.10	1.26	2.27
<b>OGBN-Pr</b>	1.40	1.47	1.60	1.60	2.86
<b>OGBN-Pa</b>	39.01	46.74	46.54	40.10	78.69

**Table 10.** Size of each partition and the total size of all partitions for different datasets using Grappa's partitioning with 4 partitions. The numbers are in GB.

## 6 Related Work

**Distributed GNN Training.** Systems such as P3 [9], DistDGL [53], ROC [17], Aligraph [54], BNS-GCN [42], NeutronStar [44], AGL [50], BGL [26], and ByteGNN [52] enable distributed training. P3 minimizes input feature transfer via model parallelism in the first layer, but subsequent hidden state exchange grows costly with wider dimensions [9]. CPU-centric systems such as Dorylus [39], ByteGNN [52], and AGL [50] suffer longer runtimes than GPU-based approaches. DistDGL [53], BGL [26], and AGL reduce communication through caching and partitioning. In contrast, Grappa does not rely on communication or caching optimizations as it removes cross-partition neighbor traffic entirely.

**Multiple GPUs Training.** Recent single-node systems (MGG, Legion, XGNN, NeutronTask/NeutronTP) aggressively overlap or cache to tame PCIe/NVLink traffic [24, 35, 37, 45, 46]. In contrast, Grappa does not rely on fast interconnects, multi-GPU caches, and complex partitioning because it eliminates neighbor exchange altogether and caching overhead.

**Graph Sampling Optimizations.** GPU samplers like gSampler [12] and NextDoor [16], and CPU designs like FlashMob [47], accelerate sampling but mostly in single-machine settings. GraphSAINT [49] improves scalability via subgraph sampling with unbiased normalization, extending GraphSAGE [13]. However, all still require remote neighbor access in partitioned graphs. Grappa removes neighbor exchange entirely, correcting coverage bias with importance weighting while remaining compatible with prior optimizations.

**Precomputation / Out-of-Core.** Cluster-GCN [8] leverages METIS [18] partitions for batching, while Grappa instead forms partitions through a lightweight chunk-sweep schedule that deterministically covers cross-chunk edges across super-epochs. This sequential sweeping is simple, model-agnostic, prefetch-friendly, and avoids precomputation. Unlike systems that still exchange features or activations across partitions, Grappa communicates only gradients. MariusGNN [41] targets single-machine out-of-core

training, whereas Grappa scales capacity via distributed, phase-parallel execution without caching.

**Local Averaging & Federated GNNs.** Our gradient-only synchronization and phase-parallel execution mirror local and decentralized SGD, which reduce communication through periodic averaging while still ensuring convergence under mild conditions [23, 36]. Unlike federated GNNs, which exchange updates to address privacy and non-IID client data [25, 28, 48], Grappa focuses on system scalability and bias correction through coverage-aware scaling. These techniques naturally complement federated training and may provide a path toward more efficient and robust federated GNNs.

## 7 Conclusions

Grappa eliminates cross-partition exchange of features and activations (gradient-only communication) by training partitions in isolation and recovers accuracy via repartitioning and batch-level bias correction. It achieves better test accuracy than state-of-the-art methods on deeper models because its dropout-like nature implicitly reduces overfitting. It delivers up to 13× faster training and scales to trillion-edge graphs on commodity hardware.

**Artifact.** Grappa’s code and datasets used in the evaluation will be open-sourced upon publication of this paper.

## References

- [1] 2023. <https://snap.stanford.edu/graphsage/>.
- [2] 2023. <https://ogb.stanford.edu/docs/nodeprop/#ogbn-arxiv>.
- [3] 2023. <https://ogb.stanford.edu/docs/nodeprop/#ogbn-products>.
- [4] 2023. <https://ogb.stanford.edu/docs/nodeprop/#ogbn-papers100M>.
- [5] Konstantin Andreev and Harald Racke. 2006. Balanced graph partitioning. *Theory of Computing Systems* 39, 6 (2006), 929–939.
- [6] Zhenkun Cai, Xiao Yan, Yidi Wu, Kaihao Ma, James Cheng, and Fan Yu. 2021. DGCL: an efficient communication library for distributed GNN training. In *Proceedings of the Sixteenth European Conference on Computer Systems*. 130–144.
- [7] Jie Chen, Tengfei Ma, and Cao Xiao. 2018. Fastgcn: fast learning with graph convolutional networks via importance sampling. *arXiv preprint arXiv:1801.10247* (2018).
- [8] Wei-Lin Chiang, Xuanqing Liu, Si Si, Yang Li, Samy Bengio, and Cho-Jui Hsieh. 2019. Cluster-gcn: An efficient algorithm for training deep and large graph convolutional networks. In *Proceedings of the 25th ACM SIGKDD international conference on knowledge discovery & data mining*. 257–266.
- [9] Swapnil Gandhi and Anand Padmanabha Iyer. 2021. P3: Distributed Deep Graph Learning at Scale. In *15th USENIX Symposium on Operating Systems Design and Implementation, OSDI 2021, July 14–16, 2021, Angela Demke Brown and Jay R. Lorch (Eds.)*. USENIX Association, 551–568. <https://www.usenix.org/conference/osdi21/presentation/gandhi>
- [10] Thomas Gaudet, Ben Day, Arian R Jamasb, Jyothish Soman, Cristian Regep, Gertrude Liu, Jeremy BR Hayter, Richard Vickers, Charles Roberts, Jian Tang, et al. 2021. Utilizing graph machine learning within drug discovery and development. *Briefings in bioinformatics* 22, 6 (2021), bbab159.
- [11] Peter W Glynn and Donald L Iglehart. 1989. Importance sampling for stochastic simulations. *Management science* 35, 11 (1989), 1367–1392.
- [12] Ping Gong, Renjie Liu, Zunyao Mao, Zhenkun Cai, Xiao Yan, Cheng Li, Minjie Wang, and Zhuozhao Li. 2023. gSampler: General and Efficient GPU-based Graph Sampling for Graph Learning. In *Proceedings of the 29th Symposium on Operating Systems Principles, SOSP 2023, Koblenz, Germany, October 23–26, 2023*, Jason Flinn, Margo I. Seltzer, Peter Druschel, Antoine Kaufmann, and Jonathan Mace (Eds.). ACM, 562–578. doi:10.1145/3600006.3613168
- [13] William L. Hamilton, Zhitao Ying, and Jure Leskovec. 2017. Inductive Representation Learning on Large Graphs. In *Advances in Neural Information Processing Systems 30: Annual Conference on Neural Information Processing Systems 2017, December 4–9, 2017, Long Beach, CA, USA*, Isabelle Guyon, Ulrike von Luxburg, Samy Bengio, Hanna M. Wallach, Rob Fergus, S. V. N. Vishwanathan, and Roman Garnett (Eds.). 1024–1034. <https://proceedings.neurips.cc/paper/2017/hash/5dd9db5e033da9c6fb5ba83c7a7ebea9-Abstract.html>
- [14] Chloe Hsu, Robert Verkuil, Jason Liu, Zeming Lin, Brian Hie, Tom Sercu, Adam Lerer, and Alexander Rives. 2022. Learning inverse folding from millions of predicted structures. In *International Conference on Machine Learning*. PMLR, 8946–8970.
- [15] William James, Charles Stein, et al. 1961. Estimation with quadratic loss. In *Proceedings of the fourth Berkeley symposium on mathematical statistics and probability*, Vol. 1. University of California Press, 361–379.
- [16] Abhinav Jangda, Sandeep Polisetty, Arjun Guha, and Marco Serafini. 2021. Accelerating graph sampling for graph machine learning using GPUs. In *EuroSys ’21: Sixteenth European Conference on Computer Systems, Online Event, United Kingdom, April 26–28, 2021*, Antonio Barbalace, Pramod Bhatotia, Lorenzo Alvisi, and Cristian Cadar (Eds.). ACM, 311–326. doi:10.1145/3447786.3456244
- [17] Zhihao Jia, Sina Lin, Mingyu Gao, Matei Zaharia, and Alex Aiken. 2020. Improving the Accuracy, Scalability, and Performance of Graph Neural Networks with Roc. In *Proceedings of Machine Learning and Systems 2020, MLSys 2020, Austin, TX, USA, March 2–4, 2020*, Inderjit S. Dhillon, Dimitris S. Papailiopoulos, and Vivienne Sze (Eds.). mlsys.org. <https://proceedings.mlsys.org/book/300.pdf>
- [18] George Karypis and Vipin Kumar. 1997. METIS: A software package for partitioning unstructured graphs, partitioning meshes, and computing fill-reducing orderings of sparse matrices. (1997).
- [19] Arpandeep Khatua, Vikram Sharma Mailthody, Bhagyashree Taleka, Tengfei Ma, Xiang Song, and Wen-mei Hwu. 2023. IGB: Addressing The Gaps In Labeling, Features, Heterogeneity, and Size of Public Graph Datasets for Deep Learning Research. In *In Proceedings of the 29th ACM SIGKDD Conference on Knowledge Discovery and Data Mining (KDD ’23) (KDD ’23)*. doi:10.48550/ARXIV.2302.13522
- [20] Thomas N. Kipf and Max Welling. 2016. Semi-Supervised Classification with Graph Convolutional Networks. *CoRR* abs/1609.02907 (2016). arXiv:1609.02907 <http://arxiv.org/abs/1609.02907>
- [21] Edward Elson Kosasih and Alexandra Brintrup. 2022. A machine learning approach for predicting hidden links in supply chain with graph neural networks. *International Journal of Production Research* 60, 17 (2022), 5380–5393.
- [22] Srijan Kumar, William L Hamilton, Jure Leskovec, and Dan Jurafsky. 2018. Community interaction and conflict on the web. In *Proceedings of the 2018 world wide web conference*. 933–943.
- [23] Xiangru Lian, Ce Zhang, Huan Zhang, Cho-Jui Hsieh, Wei Zhang, and Ji Liu. 2017. Can decentralized algorithms outperform centralized algorithms? a case study for decentralized parallel stochastic gradient descent. *Advances in neural information processing systems* 30 (2017).
- [24] Zhiqi Lin, Cheng Li, Youshan Miao, Yunxin Liu, and Yinlong Xu. 2020. PaGraph: Scaling GNN training on large graphs via computation-aware caching. In *SoCC ’20: ACM Symposium on Cloud Computing, Virtual Event, USA, October 19–21, 2020*, Rodrigo Fonseca, Christina Delimitrou, and Beng Chin Ooi (Eds.). ACM, 401–415. doi:10.1145/3419111.3421281
- [25] Rui Liu, Pengwei Xing, Zichao Deng, Anran Li, Cuntai Guan, and Han Yu. 2024. Federated graph neural networks: Overview, techniques, and

challenges. *IEEE transactions on neural networks and learning systems* (2024).

[26] Tianfeng Liu, Yangrui Chen, Dan Li, Chuan Wu, Yibo Zhu, Jun He, Yanghua Peng, Hongzheng Chen, Hongzhi Chen, and Chuanxiong Guo. 2023. BGL: GPU-Efficient GNN Training by Optimizing Graph Data I/O and Preprocessing. In *20th USENIX Symposium on Networked Systems Design and Implementation, NSDI 2023, Boston, MA, April 17-19, 2023*, Mahesh Balakrishnan and Manya Ghobadi (Eds.). USENIX Association, 103–118. <https://www.usenix.org/conference/nsdi23/presentation/liutianfeng>

[27] Yang Liu, Xiang Ao, Zidi Qin, Jianfeng Chi, Jinghua Feng, Hao Yang, and Qing He. 2021. Pick and choose: a GNN-based imbalanced learning approach for fraud detection. In *Proceedings of the web conference 2021*. 3168–3177.

[28] Brendan McMahan, Eider Moore, Daniel Ramage, Seth Hampson, and Blaise Aguera y Arcas. 2017. Communication-efficient learning of deep networks from decentralized data. In *Artificial intelligence and statistics*. PMLR, 1273–1282.

[29] Richard C Murphy, Kyle B Wheeler, Brian W Barrett, and James A Ang. 2010. Introducing the graph 500. *Cray Users Group (CUG)* 19, 45–74 (2010), 22.

[30] Razvan Pascanu, Tomas Mikolov, and Yoshua Bengio. 2013. On the difficulty of training recurrent neural networks. In *International conference on machine learning*. Pmlr, 1310–1318.

[31] Adam Paszke, Sam Gross, Francisco Massa, Adam Lerer, James Bradbury, Gregory Chanan, Trevor Killeen, Zeming Lin, Natalia Gimelshein, Luca Antiga, et al. 2019. Pytorch: An imperative style, high-performance deep learning library. *Advances in neural information processing systems* 32 (2019).

[32] John Schulman, Sergey Levine, Pieter Abbeel, Michael Jordan, and Philipp Moritz. 2015. Trust region policy optimization. In *International conference on machine learning*. PMLR, 1889–1897.

[33] Marco Serafini and Hui Guan. 2021. Scalable graph neural network training: The case for sampling. *ACM SIGOPS Operating Systems Review* 55, 1 (2021), 68–76.

[34] Xiaoniu Song, Yiwen Zhang, Rong Chen, and Haibo Chen. 2023. UGACHE: A Unified GPU Cache for Embedding-based Deep Learning. In *Proceedings of the 29th Symposium on Operating Systems Principles*. 627–641.

[35] Xiaoniu Song, Yiwen Zhang, Rong Chen, and Haibo Chen. 2023. UGACHE: A Unified GPU Cache for Embedding-based Deep Learning. In *Proceedings of the 29th Symposium on Operating Systems Principles, SOSP 2023, Koblenz, Germany, October 23-26, 2023*, Jason Flinn, Margo I. Seltzer, Peter Druschel, Antoine Kaufmann, and Jonathan Mace (Eds.). ACM, 627–641. doi:10.1145/3600006.3613169

[36] Sebastian U Stich. 2018. Local SGD converges fast and communicates little. *arXiv preprint arXiv:1805.09767* (2018).

[37] Jie Sun, Li Su, Zuocheng Shi, Wenting Shen, Zeke Wang, Lei Wang, Jie Zhang, Yong Li, Wenyuan Yu, Jingren Zhou, and Fei Wu. 2023. Legion: Automatically Pushing the Envelope of Multi-GPU System for Billion-Scale GNN Training. In *2023 USENIX Annual Technical Conference, USENIX ATC 2023, Boston, MA, USA, July 10-12, 2023*, Julia Lawall and Dan Williams (Eds.). USENIX Association, 165–179. <https://www.usenix.org/conference/atc23/presentation/sun>

[38] Xianfeng Tang, Yozen Liu, Neil Shah, Xiaolin Shi, Prasenjit Mitra, and Suhang Wang. 2020. Knowing your fate: Friendship, action and temporal explanations for user engagement prediction on social apps. In *Proceedings of the 26th ACM SIGKDD international conference on knowledge discovery & data mining*. 2269–2279.

[39] John Thorpe, Yifan Qiao, Jonathan Eyolfson, Shen Teng, Guanzhou Hu, Zhihao Jia, Jinliang Wei, Keval Vora, Ravi Netravali, Miryung Kim, and Guoqing Harry Xu. 2021. Dorylus: Affordable, Scalable, and Accurate GNN Training with Distributed CPU Servers and Serverless Threads. In *15th USENIX Symposium on Operating Systems Design and Implementation, OSDI 2021, July 14-16, 2021, Angela Demke Brown and Jay R. Lorch (Eds.). USENIX Association, 495–514. <https://www.usenix.org/conference/osdi21/presentation/thorpe>*

[40] Petar Velickovic, Guillem Cucurull, Arantxa Casanova, Adriana Romero, Pietro Liò, and Yoshua Bengio. 2018. Graph Attention Networks. In *6th International Conference on Learning Representations, ICLR 2018, Vancouver, BC, Canada, April 30 - May 3, 2018, Conference Track Proceedings*. OpenReview.net. <https://openreview.net/forum?id=rJXMpikCZ>

[41] Roger Waleffe, Jason Mohoney, Theodoros Rekatsinas, and Shivararam Venkataraman. 2023. MariusGNN: Resource-Efficient Out-of-Core Training of Graph Neural Networks. In *Proceedings of the Eighteenth European Conference on Computer Systems, EuroSys 2023, Rome, Italy, May 8-12, 2023*, Giuseppe Antonio Di Luna, Leonardo Querzoni, Alexandra Fedorova, and Dushyanth Narayanan (Eds.). ACM, 144–161. doi:10.1145/3552326.3567501

[42] Cheng Wan, Youjie Li, Ang Li, Nam Sung Kim, and Yingyan Lin. 2022. BNS-GCN: Efficient Full-Graph Training of Graph Convolutional Networks with Partition-Parallelism and Random Boundary Node Sampling. In *Proceedings of Machine Learning and Systems 2022, MLSys 2022, Santa Clara, CA, USA, August 29 - September 1, 2022*, Diana Marculescu, Yuejie Chi, and Carole-Jean Wu (Eds.). mlsys.org. <https://proceedings.mlsys.org/paper/2022/hash/d1fe173d08e959397adf34b1d77e88d7-Abstract.html>

[43] Minjie Yu Wang. 2019. Deep graph library: Towards efficient and scalable deep learning on graphs. In *ICLR workshop on representation learning on graphs and manifolds*.

[44] Qiang Wang, Yanfeng Zhang, Hao Wang, Chaoyi Chen, Xiaodong Zhang, and Ge Yu. 2022. NeutronStar: Distributed GNN Training with Hybrid Dependency Management. In *SIGMOD '22: International Conference on Management of Data, Philadelphia, PA, USA, June 12 - 17, 2022*, Zachary G. Ives, Angela Bonifati, and Amr El Abbadi (Eds.). ACM, 1301–1315. doi:10.1145/3514221.3526134

[45] Yuke Wang, Boyuan Feng, Zheng Wang, Tong Geng, Kevin Barker, Ang Li, and Yufei Ding. 2023. {MGG}: Accelerating graph neural networks with {Fine-Grained} {Intra-Kernel} {Communication-Computation} pipelining on {Multi-GPU} platforms. In *17th USENIX Symposium on Operating Systems Design and Implementation (OSDI 23)*. 779–795.

[46] Jianbang Yang, Dahai Tang, Xiaoniu Song, Lei Wang, Qiang Yin, Rong Chen, Wenyuan Yu, and Jingren Zhou. 2022. GNNLab: a factored system for sample-based GNN training over GPUs. In *EuroSys '22: Seventeenth European Conference on Computer Systems, Rennes, France, April 5 - 8, 2022*, Yérém-David Bromberg, Anne-Marie Kermarrec, and Christos Kozirakis (Eds.). ACM, 417–434. doi:10.1145/3492321.3519557

[47] Ke Yang, Xiasong Ma, Saravanan Thirumuruganathan, Kang Chen, and Yongwei Wu. 2021. Random Walks on Huge Graphs at Cache Efficiency. In *SOSP '21: ACM SIGOPS 28th Symposium on Operating Systems Principles, Virtual Event / Koblenz, Germany, October 26-29, 2021*, Robbert van Renesse and Nickolai Zeldovich (Eds.). ACM, 311–326. doi:10.1145/3477132.3483575

[48] Yuhang Yao, Weizhao Jin, Srivatsan Ravi, and Carlee Joe-Wong. 2023. FedGCN: Convergence-communication tradeoffs in federated training of graph convolutional networks. *Advances in neural information processing systems* 36 (2023), 79748–79760.

[49] Hanqing Zeng, Hongkuan Zhou, Ajitesh Srivastava, Rajgopal Kannan, and Viktor K. Prasanna. 2020. GraphSAINT: Graph Sampling Based Inductive Learning Method. In *8th International Conference on Learning Representations, ICLR 2020, Addis Ababa, Ethiopia, April 26-30, 2020*. OpenReview.net. <https://openreview.net/forum?id=BJe8pkHFwS>

[50] Dalong Zhang, Xin Huang, Ziqi Liu, Jun Zhou, Zhiyang Hu, Xianzheng Song, Zhibang Ge, Lin Wang, Zhiqiang Zhang, and Yuan Qi. 2020. AGL: A Scalable System for Industrial-purpose Graph Machine Learning. *Proc. VLDB Endow.* 13, 12 (2020), 3125–3137. doi:10.14778/3415478.3415539

- [51] Kai Zhao, Yukun Zheng, Tao Zhuang, Xiang Li, and Xiaoyi Zeng. 2022. Joint learning of e-commerce search and recommendation with a unified graph neural network. In *Proceedings of the Fifteenth ACM International Conference on Web Search and Data Mining*. 1461–1469.
- [52] Chenguang Zheng, Hongzhi Chen, Yuxuan Cheng, Zhezheng Song, Yifan Wu, Changji Li, James Cheng, Hao Yang, and Shuai Zhang. 2022. ByteGNN: Efficient Graph Neural Network Training at Large Scale. *Proc. VLDB Endow.* 15, 6 (2022), 1228–1242. doi:10.14778/3514061.3514069
- [53] Da Zheng, Chao Ma, Minjie Wang, Jinjing Zhou, Qidong Su, Xiang Song, Quan Gan, Zheng Zhang, and George Karypis. 2020. DistDGL: Distributed Graph Neural Network Training for Billion-Scale Graphs. *CoRR* abs/2010.05337 (2020). arXiv:2010.05337 <https://arxiv.org/abs/2010.05337>
- [54] Rong Zhu, Kun Zhao, Hongxia Yang, Wei Lin, Chang Zhou, Baole Ai, Yong Li, and Jingren Zhou. 2019. Aligraph: A comprehensive graph neural network platform. *arXiv preprint arXiv:1902.08730* (2019).

## Appendix

### A Proof of Theorem 3.1

**Theorem.** Under assumption (5) and if  $\left| \frac{p_v(u)}{q_v^t(u)} \nabla_\theta g_v(u) \right| \leq M$  for some constant  $M$  and  $S_{\mathcal{D}}^t$  and  $S_{\mathcal{D}_v}^{local}$  are i.i.d. samples,

$$\lim_{T \rightarrow \infty} \mathbb{E} [\nabla_\theta \tilde{L}^{corr}] = \nabla_\theta L \quad (13)$$

*Proof.* By i.i.d. sampling, we have:

$$\mathbb{E} [\nabla_\theta \tilde{L}^{corr}] = \frac{1}{T} \sum_{t=1}^T \mathbb{E}_{v \sim \mathcal{D}} \left[ \mathbb{E}_{u \sim \mathcal{D}_v^{local}} \left[ \frac{p_v(u)}{q_v^t(u)} \nabla_\theta g_v(u) \right] \right] \quad (14)$$

By the dominated convergence theorem and assumption (5), we have:

$$\begin{aligned} \lim_{T \rightarrow \infty} \frac{1}{T} \sum_{t=1}^T \mathbb{E}_{v \sim \mathcal{D}} \left[ \mathbb{E}_{u \sim \mathcal{D}_v^{local}} \left[ \frac{p_v(u)}{q_v^t(u)} \nabla_\theta g_v(u) \right] \right] = \\ \mathbb{E}_{v \sim \mathcal{D}} \left[ \mathbb{E}_{u \sim \mathcal{D}_v^{local}} \left[ \frac{p_v(u)}{q_v(u)} \nabla_\theta g_v(u) \right] \right] \end{aligned} \quad (15)$$

The result follows by applying the importance sampling theorem (3).  $\square$

### B Proof of Theorem 3.2

**Theorem.** Assuming that gradients are independently identically distributed  $\nabla_\theta g_v(u) \sim$  i.i.d with finite mean  $\mu \in \mathbb{R}^{|\theta|} \setminus \mathbf{0}$  independent of  $\frac{p_v(u)}{q_v(u)}$ , equation (9) gives the scalar  $c$  that minimizes:

$$\left\| \mathbb{E} [\nabla_\theta \tilde{L}^{corr}] - c \mathbb{E} [\nabla_\theta g_{S_{\mathcal{D}}}] \right\|_2 \quad (16)$$

*Proof.* After squaring the objective function (16), standard vector calculus gives the orthogonal projection of  $\mathbb{E} [\nabla_\theta \tilde{L}^{corr}]$  onto  $\mathbb{E} [\nabla_\theta g_{S_{\mathcal{D}}}]$ :

$$\begin{aligned} \frac{\partial}{\partial c} \left\| \mathbb{E} [\nabla_\theta \tilde{L}^{corr}] - c \mathbb{E} [\nabla_\theta g_{S_{\mathcal{D}}}] \right\|_2^2 = 0 \Rightarrow c = \\ (\mathbb{E} [\nabla_\theta g_{S_{\mathcal{D}}}]^\top \mathbb{E} [\nabla_\theta g_{S_{\mathcal{D}}}])^{-1} \mathbb{E} [\nabla_\theta g_{S_{\mathcal{D}}}]^\top \mathbb{E} [\nabla_\theta \tilde{L}^{corr}] \end{aligned} \quad (17)$$

By the assumptions of the theorem:

$$\mathbb{E} [\nabla_\theta g_{S_{\mathcal{D}}}] = \frac{1}{|S_{\mathcal{D}}|} \sum_{v \in S_{\mathcal{D}}} \frac{1}{|S_{\mathcal{D}_v}^{local}|} \sum_{u \in S_{\mathcal{D}_v}^{local}} \mu = \mu \quad (18)$$

$$\begin{aligned} \mathbb{E} [\nabla_\theta \tilde{L}^{corr}] = \frac{1}{|S_{\mathcal{D}}|} \sum_{v \in S_{\mathcal{D}}} \frac{1}{|S_{\mathcal{D}_v}^{local}|} \sum_{u \in S_{\mathcal{D}_v}^{local}} \frac{p_v(u)}{q_v(u)} \mu \\ = s_L \mu \end{aligned} \quad (19)$$

where  $s_L = \frac{1}{|S_{\mathcal{D}}|} \sum_{v \in S_{\mathcal{D}}} \frac{1}{|S_{\mathcal{D}_v}^{local}|} \sum_{u \in S_{\mathcal{D}_v}^{local}} \frac{p_v(u)}{q_v(u)}$ . This gives:

$$\begin{aligned} c = (\mu^\top \mu)^{-1} \mu^\top \mu s_L = s_L = \\ \frac{1}{|S_{\mathcal{D}}|} \sum_{v \in S_{\mathcal{D}}} \frac{1}{|S_{\mathcal{D}_v}^{local}|} \sum_{u \in S_{\mathcal{D}_v}^{local}} \frac{p_v(u)}{q_v(u)} \end{aligned} \quad (20)$$

$\square$

### C Minimally-Biased Estimator Results

In the main text, we presented the results for the batch-level estimator  $\nabla_\theta \tilde{L}^{batch}(c)$  (8) with resampling-based correction factors  $c_{resampling}^t$  (12). Table 11 shows the test accuracy results for the minimally-biased estimator with equal selection probabilities for neighbors  $c_{uniform}^t$  (10). Comparing the accuracy to the results of the resampling-based estimator  $c_{resampling}^t$  (12) is inconclusive, but the resampling-based estimator has better accuracy in 10/18 cases and in all cases for the GCN architecture and is more stable. More stability is expected for an estimator that achieves shrinkage and better accuracy hints at the benefits of accepting some degree of bias to avoid overfitting.

	OGBN-Ar	Reddit	OGBN-Pr
<b>Sage-2</b>	0.5590	0.9627	0.7706
<b>GCN-2</b>	0.4629	0.8943	0.6630
<b>GAT-2</b>	0.5640	0.9483	0.7874
<b>Sage-3</b>	0.5529	0.9611	0.7815
<b>GCN-3</b>	0.4433	0.8414	0.6919
<b>GAT-3</b>	0.5714	0.9083	0.7786

**Table 11.** Test accuracy for the minimally-biased gradient estimator  $\nabla_\theta \tilde{L}^{batch}(c)$  (8) with correction factors for a uniform neighbor distribution  $c_{uniform}^t$  (10).

### D Convergence behavior

We evaluate the convergence of each system in a selected subset of scenarios from Table 3. We pick GCN-2 as the model on the OGBN-Pr dataset. Figure 6 shows the evolution of the training accuracy.

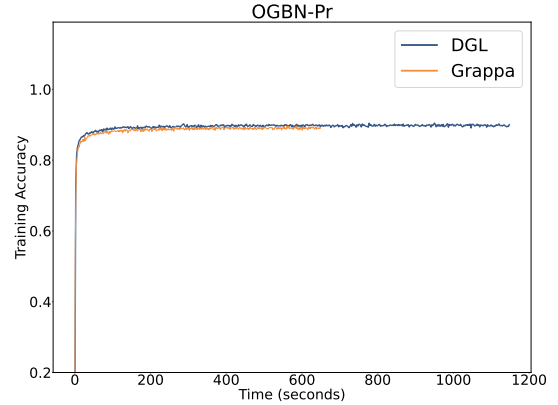


**Figure 6.** Training accuracy over time for GCN-2 with 16 partitions. Training runs for a total of 500 epochs. Both systems achieve models with near-identical test accuracy (see Table 3). The experiment uses our V100 cluster.

We observe no meaningful differences in training accuracy across systems. Moreover, in each case, the training process converges similarly and within roughly the same number of epochs. However, Grappa's epoch time is almost half of DGL's. The other models and datasets in Table 3 exhibit similar patterns.